Computers and Concrete, Vol. 11, No. 2 (2013) 149-167
DOI: http://dx.doi.org/10.12989/cac.2013.11.2.149

Stress-strain behavior and toughness of high-performance steel fiber reinforced concrete in compression

P. Ramadoss[*1] and K. Nagamani[2]

[1]*Department of Civil Engineering, Pondicherry Engineering College, Puducherry-605014, India*
[2]*Structural Engineering Division, Anna University, Chennai-600 025, India*

(Received December 25, 2011, Revised June 11, 2012, Accepted June 25, 2012)

Abstract. The complete stress-strain behavior of steel fiber reinforced concrete in compression is needed for the analysis and design of structures. An experimental investigation was carried out to generate the complete stress-strain curve of high-performance steel fiber reinforced concrete (HPSFRC) with a strength range of 52–80 MPa. The variation in concrete strength was achieved by varying the water-to-cementitious materials ratio of 0.40-0.25 and steel fiber content (Vf = 0.5, 1.0 and 1.5% with l/d = 80 and 55) in terms of fiber reinforcing parameter, at 10% silica fume replacement. The effects of these parameters on the shape of stress-strain curves are presented. Based on the test data, a simple model is proposed to generate the complete stress-strain relationship for HPSFRC. The proposed model has been found to give good correlation with the stress-strain curves generated experimentally. Inclusion of fibers into HPC improved the ductility considerably. Equations to quantify the effect of fibers on compressive strength, strain at peak stress and toughness of concrete in terms of fiber reinforcing index are also proposed, which predicted the test data quite accurately. Compressive strength prediction model was validated with the strength data of earlier researchers with an absolute variation of 2.1%.

Keywords: compressive strength; high-performance concrete; crimped steel fiber; fiber reinforcing index; stress-strain curve; toughness; modeling

1. Introduction

Steel fiber reinforced concrete (SFRC) is increasingly used as a structural material, has gained acceptance for a variety of applications, namely industrial floors, bridge decks, pavement, hydraulic and marine structures, nuclear vessels, repair and rehabilitation works, blast resistance and penetration resistance structures (Balaguru and Shah 1992, ACI 544.1R-96, ACI 544.4R-89). The compressive strength is normally specified for structural applications while flexural strength is normally specified for pavement applications. In certain applications, toughness parameters may be specified (ACI 544.3R-1993).

In the production of HSC/HPC, silica fume plays a vital role because of the significant improvement attained on the interfacial zone of cement paste- aggregate due to the increased bond, which makes the interfacial zone more dense (Aitcin 1998). HPC achieved by using silica fume leads to the densification of the concrete, which usually combines high–strength with high

[*]Corresponding author, Associate Professor, E-mail: dosspr@pec.edu

durability. On the other hand the use of steel fibers has a great contribution to concrete by improving its ductility. Therefore, both the silica fume and steel fiber are inevitable materials to be used for a more ductile high-strength/ high-performance concrete. The improved toughness in compression imparted by fibers is useful in preventing sudden and explosive failure under static loading, and in absorption of energy under dynamic loading (ACI 544.4R-1989). Recent studies have shown increasing evidence that the brittle nature of HSC/HPC can be overcome by the addition of discrete fibers of small diameter in the concrete mix (Hsu and Hsu 1994, Mansur *et al.* 1999). To incorporate such improvement in structural design, it is necessary to establish the complete stress-strain characteristics of the resulting fibrous concrete. To design and analyze the structure using HPSFRC, the stress-strain response of the material in compression is needed.

The previous researchers (Wang *et al.* 1987, Carreira and Chu 1985, Wee *et al.* 1996) have proposed a number of empirical expressions for the stress-strain curve of plain concrete. However they can't represent the behavior of SFRC. Ezeldin and Balaguru (1992) have proposed an analytical expression for generating the stress-strain curve of steel fiber reinforced concrete based on the expression proposed by Carreira and Chu (1985) for uniaxial compression of plain concrete. This expression involves a material parameter β (a non-dimensional parameter), which is to be evaluated from the physical property of the stress-strain curve. It has been noticed from the experimental results that the fibers have more effective contribution on the compressive stress-strain curve in the post failure region. Hence, using the experimental results, a best fitting analysis was performed to obtain a relation between the parameter β and RI based on the physical property of the stress-strain curve, which is the slope of the inflection point at the descending segment. The equation proposed by Carreria and Chu (1985) is a generalized form of serpentine curve, in which 'β' is a material parameter that depends on the shape of the stress-strain curve. To model various descending branches of the stress-strain curve for SFRC, four different sets of constants used are related to the peak stress and strain at peak stress, to the stress and strain at 45% of the peak stress (modulus of elasticity), to the stress and strain at the inflection point and to the stress and strain of 0.0154 at an arbitrary point taken at the tail end of the descending branch.

Hsu and Hsu (1994) have modified an empirical equation proposed by Carriera and Chu (1985), and again used by Ezeldin and Balaguru (1992), to investigate the Stress-strain characteristics for both plain and high strength fiber concrete under compression. They used the parameters β and 'n' as the material parameters. β depends on the shape of the stress-strain diagram, and 'n' depends on the strength of material. The parameter 'n' has been introduced to importantly effect the descending portion of the stress-strain curve of high strength fiber concrete. Earlier researchers (Ezheldin and Balaguru 1992, Hsu and Hsu 1994, Chin *et al.* 1997, Mansur *et al.* 1999, Nataraja *et al.* 1999, Campione and Mendola 2004, Haktanir *et al.* 2006, Bhargava *et al.* 2006, Kittinun *et al.* 2010, Zongjin and Yanhua 2010, Wang *et al.* 2008, Williams *et al.* 2010) investigated the effect of inclusion of discrete steel fibers on the stress-strain relationship of concrete. Bang *et al.* (2010) and Wang *et al.* (2008) have studied the stress-strain behavior of SFRC. A few research studies exist on the behavior of HSC/HPC, and analytical modeling of stress-strain relationship of high-strength SFRC with silica fume is particularly lacking.

Ramesh *et al.* (2003) have shown that columns cast with suitable randomly distributed fibers show excellent performance comparing to specimens cast without fibers, particularly with respect to post-peak failure. Such a study revealed that fibers provide indirect confinement to the concrete. Stress-strain curves of FRC show an appreciable increase in strain at the peak stress and substantially higher toughness which is the measure of ability to absorb energy.

In the present study, this paper deals with complete stress-strain behavior of high-performance steel fiber reinforced concrete with compressive strength ranging from 52-80 MPa. Crimped steel fibers of three volume fractions of 0.5, 1.0 and 1.5% (39, 78 and 117.5 kg/m^3, respectively) with the aspect ratios of 80 and 55 were used. The variation in concrete strength was achieved by varying the w/cm ratio with 10% silica fume replacement. The influence of fiber addition in terms of fiber reinforcing index on peak compressive stress, strain at peak stress and toughness of concrete, initial tangent modulus, secant modulus, and nature of stress-strain curve, and modulus of rupture were investigated. Based on the test data, analytical model has been developed to fit the post-peak softening behavior and for generating complete stress-strain (σ-ε) curves for high-performance concrete reinforced with crimped steel fibers.

2. Research significance

The stress-strain behavior of the constituent material in predicting the behavior of reinforced concrete structures is the fundamental requirement. If the behavior of concrete in uniaxial compression is known, its flexural behavior can also be predicted. The use of fibers are becoming popular in earthquake resistance structures/infrastructures where, ductility of the materials to appreciably enhance energy absorption capacity of the HSC/HPC columns is the prime factor, the complete stress-strain relationship of fibrous concrete is required in order to analyze and design the fiber reinforced concrete elements. However, only a few studies, that have been reported in the literature on stress-strain behavior of high-strength/ high-performance SFRC. An attempt has been made in the present study to obtain complete stress-strain curves and to develop analytical model for the behavior of HPSFRC in compression under uniaxial loading.

3. Experimental program

3.1 Materials, mixture proportions and preparation of specimens

Ordinary Portland cement- 53 grade conforming to IS: 12269–1987 with a 28-day compressive

Table 1 Chemical composition and physical properties of OPC- 53 grade

Chemical composition (in percentage)									
CaO	SiO_2	AlO_3	Fe_2O_3	Mg O	K_2O	SO_3	P_2O_5	LOI	LSF
64.26	21.07	5.54	5.16	0.86	0.37	0.72	0.33	1.54	0.925

Physical properties			
Specific gravity, S_g	B.E.T. Fineness (m^2/kg)	Soundness by Le-Chatelier expansion (mm)	28-day compressive strength (MPa)
3.15	245	5	54.5

Table 2 Chemical analysis of silica fume (Grade 920-D)

Silicon dioxide, SiO_2	Moisture content	Loss of Ignition @ 975° C	Carbon	Fineness (by residue on 45μ)
88.7%	0.7%	1.8%	0.9%	2%

strength of 54.5 MPa and condensed silica fume (in a powder form), having fineness by specific surface area of 23000 m^2/kg, a specific gravity of 2.75 were used. The chemical and physical properties of OPC and chemical analysis of silica fume (Grade 920-D) are given in Tables 1 and 2, respectively.

Fine aggregate of locally available river sand passing through 4.75 mm IS sieve, conforming to grading zone-II of IS: 383-1978 was used. Sand has fineness modulus of 2.65, a specific gravity of 2.63 and water absorption of 0.98%. Coarse aggregate of crushed blue granite stones with 12.5 mm maximum size, conforming to IS: 383-1978 was used. The characteristics of coarse aggregate are: Specific gravity = 2.70, Fineness modulus = 6.0, Dry rodded unit weight = 1600 kg/m^3 and Water absorption = 0.65%.

Super-plasticizer of sulphonated naphthalene formaldehyde (SNF) condensate as HRWR admixture conforming to ASTM Type F (ASTM C494) and IS: 9103-1999 which has a specific gravity of 1.20, was used.

Fibers conforming to ASTM A820-01 have been used in this investigation, are crimped steel fibers (undulated) of length = 36/ 25 mm and diameter = 0.45 mm, with the aspect ratios of 80 and 55, having an ultimate tensile strength, f_u of 910 MPa.

Table 3 Mix proportions (data for 1 m^3) and Ultrasonic pulse velocity measurements for HPSFRC

Mix designation	W/Cm	C, kg	FA, kg	CA, kg	SF, kg	Steel fiber, V_f(%)	SP, kg	UPV m/sec.
FC1-0	0.4	394.2	691	1088	43.8	0	7.66	4524
FC1-0.5	0.4	394.2	687	1079	43.8	0.5	7.66	4326
FC1-1	0.4	394.2	682	1071	43.8	1.0	7.66	4267
FC1-1.5	0.4	394.2	678	1062	43.8	1.5	7.66	4098
FC2-0	0.35	437.4	664	1088	48.6	0	9.72	4504
FC2-0.5	0.35	437.4	660	1079	48.6	0.5	9.72	4405
FC2-1	0.35	437.4	655	1071	48.6	1.0	9.72	4216
FC2-1.5	0.35	437.4	651	1062	48.6	1.5	9.72	4196
FC3-0	0.3	495	624	1088	55	0	13.75	4559
RC3-0.5	0.3	495	620	1079	55	0.5	13.75	4451
FC3-1	0.3	495	615	1071	55	1.0	13.75	4335
FC3-1.5	0.3	495	611	1062	55	1.5	13.75	4187
FC4-0	0.25	576	562	1088	64	0	17.60	4322
FC4-0.5	0.25	576	558	1079	64	0.5	17.60	4219
FC4-1	0.25	576	553	1071	64	1.0	17.60	4120
FC4-1.5	0.25	576	549	1062	64	1.5	17.60	4026

In mix designation FC1 to FC4, silica fume replacement is 10 percent by weight of cementitious materials, after hyphen ssdenotes fiber volume fraction in percent.
Water present in Super plasticizer is excluded in calculating the water to cementitious materials ratio. Water content for mixes FC1, FC2, FC3 and FC4 is 175, 170, 165 and 160 kg, respectively.
V_f(%) denotes Steel fiber volume fraction in percent in total volume of concrete.
UPV denotes Ultrasonic pulse velocity in m/sec.

Mixtures were proportioned using guidelines and specifications given in ACI 211.1–1991 and ACI 211.4R–93, and recommended guidelines of ACI 544.3R-1993. Mixture proportions used in this test programme are listed in Table 3. This aspect of work was carried out elsewhere (Ramadoss and Nagamani 2008). For each water-cementitious materials ratio, 3 fibrous concrete mixes were prepared having fiber volume fractions, V_f of 0.5, 1.0 and 1.5 percent by volume of concrete (39, 78 and 117.5 kg/m^3). Super-plasticizer with dosage range of 1.75 to 2.5% by weight of cementitious materials has been used to maintain the adequate workability of plain and fiber reinforced concrete.

16 series of steel fiber reinforced concrete mixes with an aspect ratio of fiber as 80, and 8 series of concrete mixes with an aspect ratio of fiber as 55 (for verification of strength model) were used in this investigation. Concrete was mixed using a tilting type mixer and specimens were cast using steel moulds, compacted by table vibrator. For each mix at least three 150 mm diameter cylinders and three 100 x 100 x 500 mm prisms were produced. Specimens were demoulded after 24 hours of casting and all the specimens were cured in the same curing tank water at 27±2^{o}C until the age of testing at 28 days.

3.2 Testing for strength

Table 4 Experimental and calculating results for fiber reinforced concrete and plain concrete

Mix designa-tion	RI	Experimental values						Calculated values			
		f'_{cf} MPa	f_{rf} MPa	ϵ_o (mm/mm)	E_{it} GPa	TR	E_c GPa	f'_{cf} MPa	ϵ_o	E_{it} GPa	TR
FC1-0	0	52.56	6.21	0.00260	31.308	0.2038	29.68	52.56	0.0026	35.484	0.204
FC1-0.5	1.29	54.77	7.15	0.00305	34.583	0.6276	30.14	54.36	0.0028	36.673	0.391
FC1-1	2.58	56.01	7.73	0.00320	35.664	0.6574	30.92	56.16	0.0029	37.335	0.579
FC1-1.5	3.88	57.40	8.19	0.00330	37.806	0.6715	31.78	57.98	0.0031	38.075	0.768
FC2-0	0	55.85	6.75	0.00305	34.397	0.2161	30.87	55.85	0.0031	37.250	0.216
FC2-0.5	1.29	59.65	8.06	0.00325	38.260	0.6194	32.32	57.65	0.0032	39.264	0.404
FC2-1	2.58	61.05	8.54	0.00338	39.423	0.6386	33.26	59.45	0.0034	40.000	0.591
FC2-1.5	3.88	61.44	9.15	0.00345	41.826	0.6647	33.97	61.27	0.0035	40.204	0.780
FC3-0	0	63.86	7.40	0.00335	39.919	0.2252	34.14	63.86	0.0034	41.466	0.225
FC3-0.5	1.29	67.12	8.76	0.00335	43.961	0.6642	35.96	65.66	0.0035	43.151	0.413
FC3-1	2.58	68.91	9.32	0.00365	44.328	0.6642	36.52	67.46	0.0037	44.069	0.600
FC3-1.5	3.88	69.67	10.13	0.00370	46.753	0.6851	36.98	69.28	0.0038	44.457	0.789
FC4-0	0	74.87	8.02	0.00360	48.068	0.2454	37.65	74.87	0.0036	47.093	0.245
FC4-0.5	1.29	77.42	9.58	0.00376	49.778	0.6462	39.47	76.67	0.0038	48.371	0.433
FC4-1	2.58	79.96	10.36	0.00388	51.032	0.6469	40.52	78.47	0.0039	49.637	0.621
FC4-1.5	3.88	80.41	11.01	0.00395	52.553	0.6789	41.06	80.29	0.0041	49.860	0.810

f'_{cf} = 150x300mm cylinder compressive strength of HPFRC, (MPa)
f_{rf}= flexural strength of HPFRC (MPa), E_{it}= initial tangent modulus (GPa), E_c = secant modulus (GPa) and TR= toughness ratio.
Fiber reinforcing index (RI) = w_f *(l/d) and average density of HPFRC = 2415 kg/m^3
Weight fraction (w_f) = (density of fiber/ density of fibrous concrete)* V_f
Aspect ratio (l/d) = length of fiber/diameter of fiber.

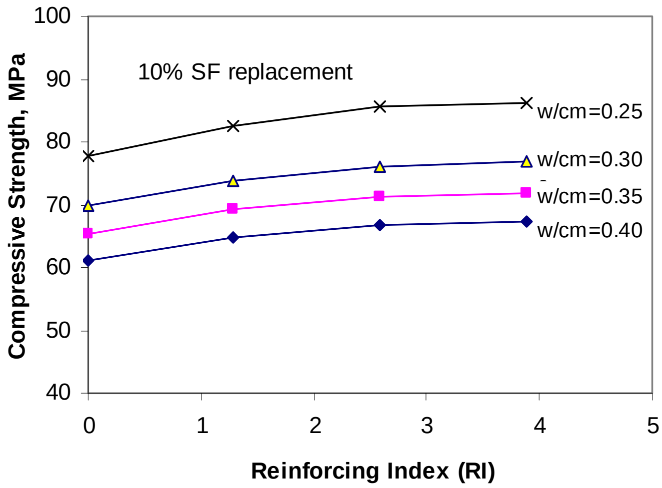

Fig. 1 Effect of fiber reinforcing index (RI) on compressive strength, MPa (10% silica fume replacement, l/*d* = 80)

3.2.1 Compressive strength

Compressive strength tests were performed according to ASTM C 39-92 standards using 150 mm diameter cylinders loaded uniaxially. Before testing, the cylinders were capped with a hard plaster on the cast faces to ensure parallel loading faces of the test specimens and constant height for all cylinders. A compressometer equipped with dial gauges available in the laboratory was used to record the deformation of the cylinder. Efforts were made to take as many readings as possible, to get considerable length of post-peak portion of the stress-strain curve. In the descending portion readings were taken at random intervals. Stresses and corresponding strains were evaluated and average values are reported with the compressive strength ranges from 52 to 80 MPa, are given in Table 4.

3.2.2 Flexural strength

The flexural strength (Modulus of rupture) tests were conducted as per the specification of ASTM C 78-92 using 100 x 100 x 500 mm beams under third-point loading on a simply supported span of 400 mm. The tests were achieved in a 100 kN closed loop deflection controlled testing machine. Samples were tested at a deformation rate of 0.1 mm/min. Three samples (in few cases 4 or 5) were used for computing the average strength of concrete mix. Modulus of rupture obtained for HPSFRC mixes is in the range of 3.21 to 11.01 MPa, shown in Table 4. The maximum increase in tensile strength due to the addition of steel fibers was found to be about 38% in HPC mixes. This is the primary justification for using fibers in concrete matrix. The post cracking response is significantly enhanced due to the fiber bond effect in concrete matrix.

4. Results and analysis

The shape of the stress-strain curve in uniaxial compression is strongly affected by the testing conditions (stiffness of the testing machine, size and shape of the specimen, etc.) and concrete characteristics (w/cm ratio, aggregate type, fiber type and aspect ratio). To minimize the testing condition effects, careful attention was exercised to avoid variations in the testing setup and specimen's instrumentation. Ultrasonic pulse velocity measurements show the HPFRC mixes having uniform mixing, compaction and fiber distribution (Table 3).

The stress-strain relationship of concrete essentially consists of two distinct branches- an ascending branch up to the peak stress followed by a descending branch until the concrete crushes. The key parameters that are normally used to characterize the ascending branch of the curve are the initial tangent modulus, the compressive strength and the strain at peak stress. Modulus of elasticity, E_c (represents the secant modulus of elasticity at $0.45f'_c$) to define the stress-strain relationship and used as an important parameter in the analysis and design of structural elements is also required. The various mechanical properties obtained from the test results and respective stress-strain curve, and the average values for each group of specimens are presented in Table 4.

4.1 Compressive strength (f_o)

The variation in concrete strength was achieved by varying the water-to-cementitious materials ratio and fiber volume fraction, at 10% silica fume replacement. The peak stress (compressive strength) f_o or f'_{cf} and the corresponding strain ε_0 depend on the response of the specimen at or near the ultimate load. At this stage, cracks will form in the specimen due to lateral expansion of the concrete. These cracks will be directed parallel to the direction of loading. Fibers aligned normal to the loading direction will therefore be intercepted by these cracks and offer some resistance to their growth. The effect of fibers on the compressive strength of concrete (as a function of fiber reinforcing index) with varying w/cm ratio may be evaluated from Fig. 1. It may be seen that inclusion of fibers results in moderate increase in compressive strength (~10% higher than the corresponding plain concrete strength). The compressive strength of HPSFRC with fiber aspect ratio of 55 obtained for testing the model and predicted values with an absolute variation of 2.53% are presented in Table 5.

Table 5 28-day compressive strength of high-performance fiber reinforced concrete and their percentage variations (l/d of fiber = 55)

Mix designation	w/cm	RI	150 mm diameter cylinder		
			Experimental value	Predicted by Eq. (4)	Error (%)
			f_c, MPa	f_c, MPa	
FC1*-0	0.4	0	52.56	52.56	0.00
FC1*-0.5	0.4	0.86	55.21	53.76	2.62
FC1*-1	0.4	1.71	55.75	54.95	1.44
FC1*-1.5	0.4	2.57	58.46	56.15	3.95
FC3*-0	0.3	0	63.86	63.86	0.00
FC3*-0.5	0.3	0.86	67.45	65.06	3.54
FC3*-1	0.3	1.71	68.99	66.25	3.97
FC3*-1.5	0.3	2.57	70.78	67.45	4.70

Absolute variation (%) 2.53

4.2 Strain at peak stress (ε_o)

The strain at peak stress, ε_o for each specimen is plotted against the respective compressive strength and normalized stress-strain curves are shown in Figs. 2-6. The variation of strain corresponding to peak stress with respect to reinforcing index is presented in Table 4. In general, the strain at peak stress increases from 0.002 to 0.003 mm/mm with an increase in concrete strength from 52 to 80 MPa.

4.3 Initial tangent modulus (E_{it})

The initial tangent modulus E_{it} (i.e., the slope of the stress-strain (σ–ε) curve at origin) depicts the initial response of the specimen under compressive load. In this study analytical expressions should be obtained that describe the complete stress-strain curves of the fibrous concrete. Based on the experimental values, using least square regression analysis, the following expression obtained for the initial tangent modulus, $E_{it.}$

$$E_{it} = 1491.1\, f_o^{\,0.8} \quad (r{=}0.95) \quad \text{(for 150 x 300 mm cylinder)} \tag{1}$$

where initial tangent modulus E_{it} and compressive strength f_o are all expressed in MPa. Eq. (1) is valid for V_f up to1.5% by weight of concrete. The values predicted by Eq. (1) are comparable with the values estimated by the equation proposed for high-strength concrete by Mansur *et al.* (1999).

4.4 Modulus of elasticity (secant modulus) (E_c)

Modulus of elasticity (Secant modulus) was defined (according to ACI Building code -ACI 318-95) as the slope of the line drawn from a stress of zero to a compressive stress of $0.45\, f'_c$.

According to ACI 318-95, Modulus of elasticity, E_c for normal weight concrete shall be taken as $E_c = 4700 \sqrt{f'_c}$ in MPa.

Based on the correlation of data, ACI committee 363 (ACI 363R-92, State–of–the–art–report on HSC) have given the following expression for modulus of elasticity E_c for normal weight concrete:

$E_c = 3320 \sqrt{f'_c} + 6900$ in MPa. 21 MPa < f'_c < 83 MPa. (for medium or high strength concrete).

The static modulus of elasticity obtained for various concrete mixes from the respective stress-strain curve is in the range of 29.68 x 10^3 - 41.06 x 10^3 MPa, presented in Table 4.

Based on the experimental values, using least square regression analysis, the following expression was obtained for the secant elastic modulus, $E_{c.}$

$$E_c = 23077\, f_o^{\,0.65} \qquad (R = 0.99) \tag{2}$$

where secant modulus E_c and compressive strength f_o are all expressed in MPa.

The Eq. (2) gives the lower bound values for the steel fiber reinforced concretes to that of ACI 318-1995, ACI 363-1992 and IS: 456-2000 recommended equations. On comparing the CEB-FIP model code for concrete structure (1991) and BS code (BS: 8110) formulae for modulus of elasticity, the proposed formula for modulus of elasticity gives the upper bound values.

4.5 Stress–strain curves

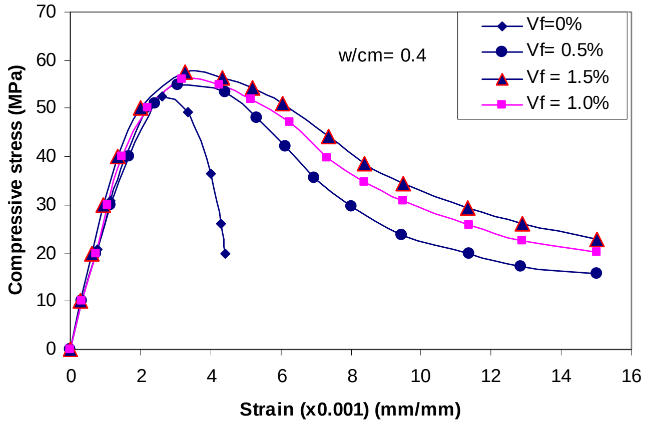

Fig. 2 Typical stress-strain curves for silica fume concrete and steel fiber reinforced concrete (*w*/cm = 0.40, SF content=10%)

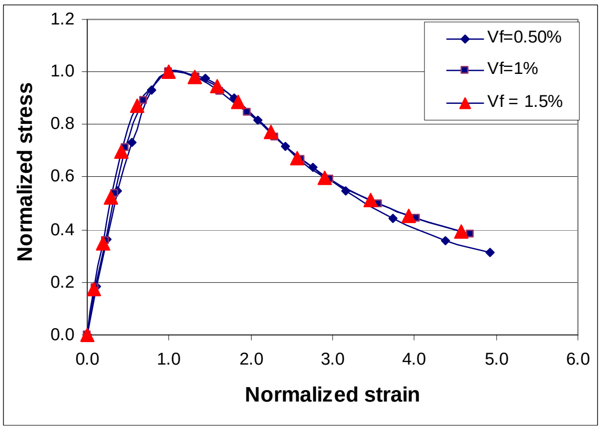

Fig. 3 Effect of fiber volume fraction on the normalized stress-strain curves (*w*/cm=0.40, SF content=10%)

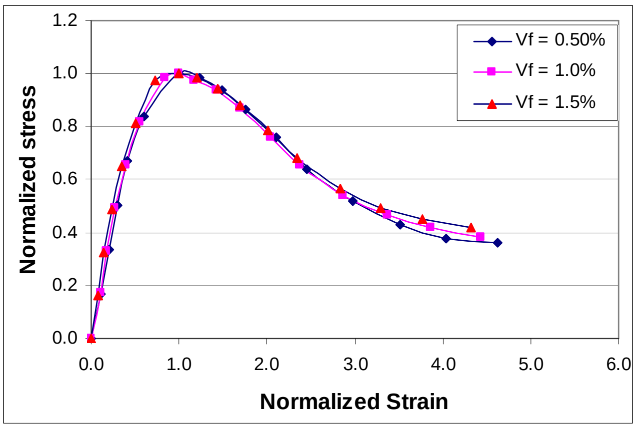

Fig. 4 Effect of fiber volume fraction on the normalized stress-strain curves (*w*/cm=0.35, SF content=10%)

The stress–strain behavior of HPSFRC with compressive strength ranging from 52 to 80 MPa has been investigated. The typical stress-strain curve for HPC (plain) and SFRC is shown in Fig. 2. Figs. 3-6 show the normalized stress-strain (σ–ε) curves for high-performance fiber reinforced concrete in compression with different fiber volume fraction (V_f). It clearly shows that the post-peak segment of the σ–ε curve is affected by the addition of steel fibers. From the stress–strain curves generated in this study, it can be observed that an increase in concrete strength increases the extent of curved portion in ascending branch and renders the drop in the descending part steeper for HPC and gradually flatter for SFRC. Although the drop in the post peak region is gradual for SFRC, there is a residual stress even at a strain as high as 0.015. An increasing in the slope of the descending part of the stress-strain curve is also observed by increasing the fiber volume fraction. The gradual change in shape with an increase in strength have, however, been reported on by many investigators in the past. Actual stress-strain curves (σ–ε) and Normalized stress-strain curves between f_c/f'_{cf} and $\varepsilon/\varepsilon_o$, for different fibrous concretes are shown in Fig. 2 and Figs. 3-6, respectively.

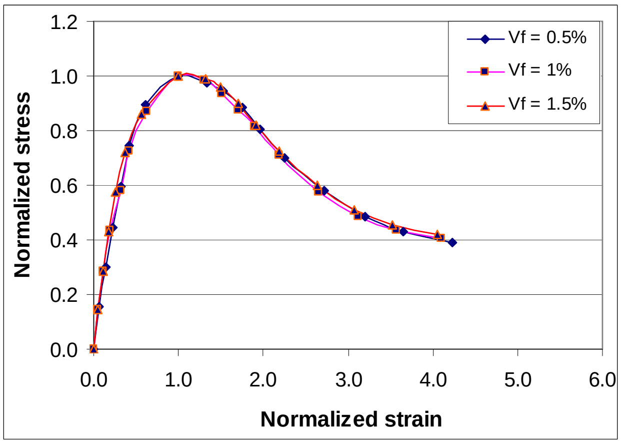

Fig. 5 Effect of fiber volume fraction on the normalized stress-strain curves (*w*/cm=0.30, SF content=10%)

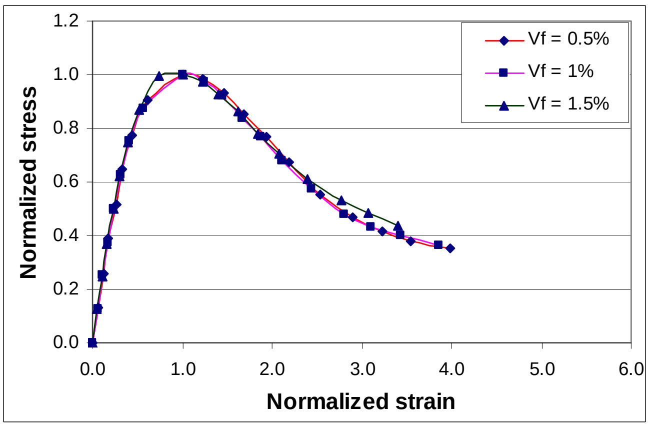

Fig. 6 Effect of fiber volume fraction on the normalized stress-strain curves (*w*/cm=0.25, SF content=10%)

4.6 Compressive toughness

Toughness is a measure of the capability of the material to absorb energy during deformation when subjected to compressive load, estimated using the area under stress-strain curve. The energy absorption per unit volume under compression is expressed mathematically as

$$\text{Toughness} = \int^{\varepsilon} \sigma . d\varepsilon$$

The convenient way to quantify ductility is to use toughness ratio (TR) (refer Fig. 7).

$$\text{TR} = \frac{Area(OABC)}{f'_{cf}\, x 0.015} \tag{3}$$

Ezheldin and Balaguru (1992) have proposed a rigid plastic approach to define the toughness ratio. In the results presented in this paper, the toughness is measured as the total area under stress-strain curve up to a strain of 0.015 mm/mm, which is five times the ultimate concrete strain of 0.003 mm/mm as adopted in the ACI building code for concrete structures (ACI 318-95). Ezheldin and Balaguru (1992) have also used an ultimate strain of 0.015 for computing the toughness as it is sufficient to represent the trend of post peak behavior of SFRC. This toughness is compared to the toughness of a rigid plastic material in the form of toughness ratio (TR) as indicated in Fig. 7. It is observed in the present investigation that the area under stress-strain curve increases with the increase in fiber content, and fiber type and geometry. The fiber reinforcing index (RI = w_f*(l/d)) can be used as the fiber reinforcing parameter with weight fraction (w_f) approximately equal to 3.27 times the volume fraction. The increase in fiber reinforcing index, RI would yield a large area under the stress-strain curve making a flatter descending part and a higher toughness ratio as shown in Figs. 3-6. The toughness ratios evaluated from the stress-strain curves and the calculated values are presented in Table 4. Toughness ratio (TR_f) of SFRC as function of fiber reinforcing index and toughness ratio of HPC is shown in Fig. 14. Nataraja *et al.* (1999) have obtained maximum toughness ratio of 0.77 for SFRC with w/c = 0.38 and RI = 2.67, which is comparable with the experimentally calculated maximum value of 0.6 for SFRC with RI= 3.88.

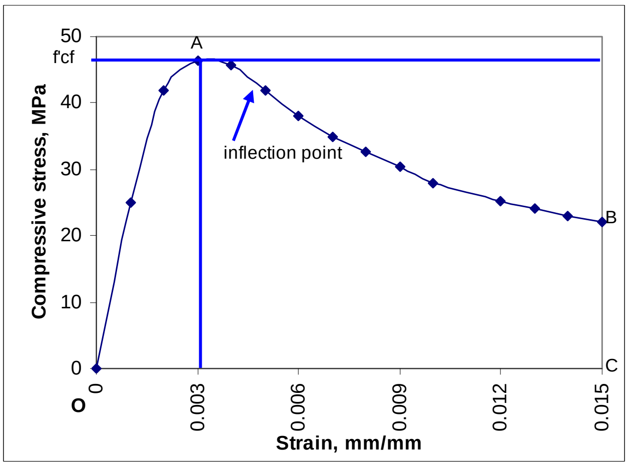

Fig. 7 Toughness ratio computation for fiber reinforced concrete

A least square regression analysis was performed using the experimental data to establish a possible relationship between the fiber-reinforcing index and the peak compressive strength, strain corresponding to peak stress, and the toughness of the concrete based on the stress-strain behavior of HPFRC mixes. All these equations well quantify the effect of fibers on compression behavior of HPFRC in terms of fiber reinforcing parameter. Results of these equations are presented in Table 5, which are based on Eqs. 4-6. The proposed equations from the complete stress-strain response of the high-performance steel fiber reinforced concrete for compressive strength ranging from 52 to 80 MPa are given below.

Compressive strength ($f_0 = f'_{cf}$)

$$f'_{cf} = f_c + 1.397\,(RI) \qquad (R = 0.95) \qquad (4)$$

where f_c and f'_{cf} are the compressive strength of plain (SF concrete) and steel fiber reinforced concrete, respectively in MPa. The percentage variation in absolute values has been obtained as 3.35.

Strain corresponding to peak stress (ε_o)

$$\varepsilon_o = \varepsilon + 0.000125\,(RI) \qquad (R = 0.97) \qquad (5)$$

where ε and ε_o are the strain at peak stress for plain (SF concrete) and steel fiber reinforced concrete, respectively in mm/mm.

Toughness ratio of concrete (TR_f)

$$TR_f = TR_c + 0.145\,(RI) \qquad (R = 0.78) \qquad (6)$$

where TR_f and TR_c are the toughness ratio of steel fiber reinforced concrete and plain concrete (HPC), respectively.

The comparison of the compressive strength data of previous researchers (Ezheldin and Balaguru 1992, Wafa and Ashour 1992, Trottier and Banthia 1994, Barros and Figueiras 1999, Fuat *et al.* 2008, Ismail and Riza 2011, Thomas and Ramasamy 2007) with the strength values predicted by the present model (Eq. 4) is shown in Fig. 15, and observed from the figure that model predicted the strengths quite accurately. The prediction model is comparable with the correlation equation developed by Xu and Shi (2009). The proposed equations (Eqs. 4-6) can be used to estimate the values of compressive strength, strain corresponding to peak stress and toughness ratio of HPC reinforced with steel fibers.

5. Analytical model for complete stress-strain curve

Figs. 8-13 show the normalized analytical curves for various fiber volume fractions and *w*/cm ratios. Despite the differences in peak stress, the descending branches of stress-strain curves might be seen to have approximately the same residual strength at a strain value of 0.01. This phenomenon was also reported by Wee *et al.* (1996).

In an earlier study (Wee *et al.* 1996), a number of available models of plain concrete had been assessed, and a modified Carreira and Chu (1985) equation was found to be simple, yet provided a good correlation with the test results on HSC. The same model has been chosen here for high-performance steel fiber reinforced concrete. An analysis of test data generated in this study reveals

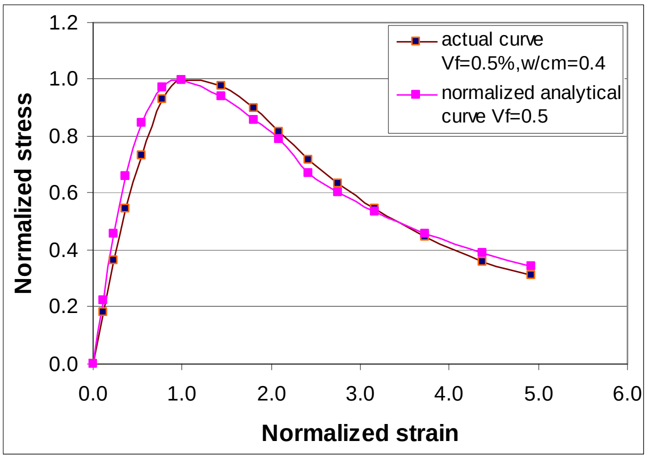

Fig. 8 Correlation of normalized actual and analytical curves (V_f=0.5% and w/cm=0.4)

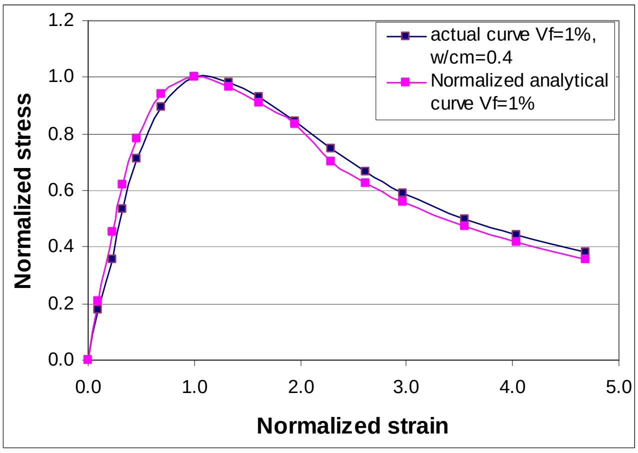

Fig. 9 Correlation of normalized actual and analytical curves (V_f=1.0% and w/cm=0.4)

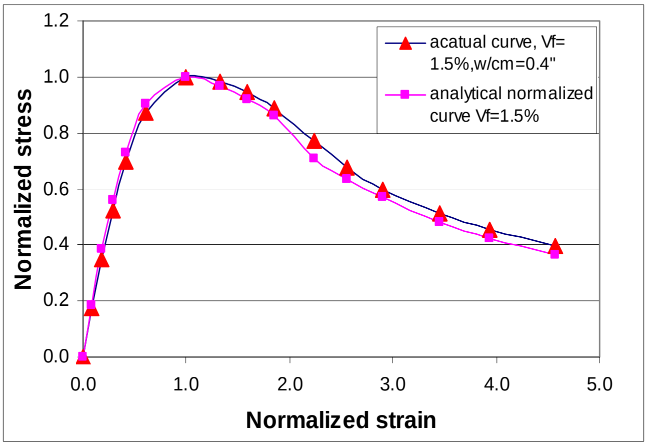

Fig. 10 Correlation of normalized actual and analytical curves (V_f=1.5% and w/cm=0.4)

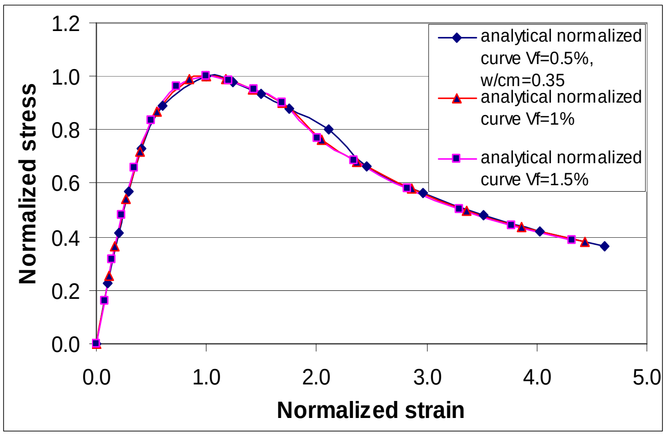

Fig. 11 Normalized analytical curves for various fiber volume fractions and *w*/cm=0.35

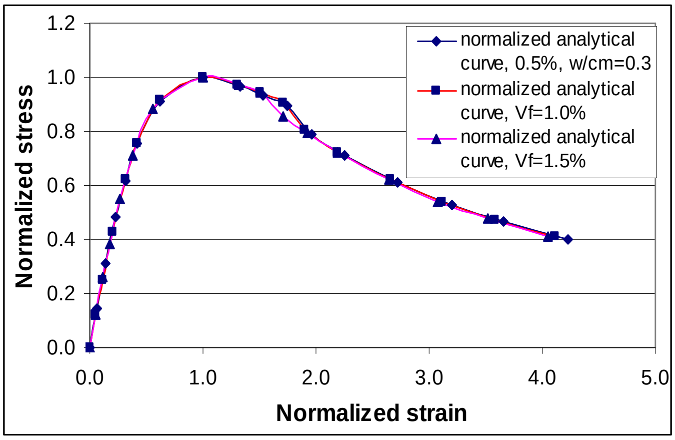

Fig. 12 Normalized analytical curves for various fiber volume fractions and *w*/cm=0.3

that the original form of the Carreira and Chu (1985) model can adequately describe the ascending branch of the curve provided appropriate values of E_{it}, f_o and ε_o are used. A modified Carreira and Chu (1985) equation is given as follows

$$\frac{f}{f_o} = \left[\frac{\beta(\varepsilon/\varepsilon_o)}{\beta - 1 + (\varepsilon/\varepsilon_o)^{\beta}} \right] \tag{7}$$

where

$$\beta = \frac{1}{1 - \dfrac{f_o}{\varepsilon_o E_{it}}} \tag{8}$$

where f_o = peak stress and β = material parameter that depends on the shape of the stress-strain curve, which is greater than or equal to 1.

Carreira and Chu (1985) equation does not adequately represent the descending portion of the curve for a wide range of concrete strength. For the descending branch of the curve, a modified equation for 'β' is introduced to reflect the effect of reinforcing parameter and to cater for the residual stress. This modified Carreira and Chu (1985) equation generates an σ-ε relationship only up to a strain value equal to 0.6 of the ultimate compressive stress in the descending portion of the stress–strain curve (Mansur *et al.* 1999). Therefore, beyond this a separate equation is required to assess the parameter 'β'.

The least square statistical analysis was performed to obtain the relationship between the parameter 'β' and RI of the fibrous concrete based on the physical properties of the σ-ε curves, which is the slope of the inflection point at the descending segment (see Fig. 2). This slope is represented by E_{ip}. The following equations were found to describe the relationships, for compressive strength ranging from 55 to 80 MPa of fibrous concrete.

$$\beta = 0.0001\, E_{ip} + 1.424, \qquad (r = 0.85) \tag{9a}$$

$$E_{ip} = 76.264\,(\mathrm{RI}) + 6825, \qquad (r = 0.98) \tag{9b}$$

$$\beta = 0.007626\,(\mathrm{RI}) + 2.1065 \tag{9c}$$

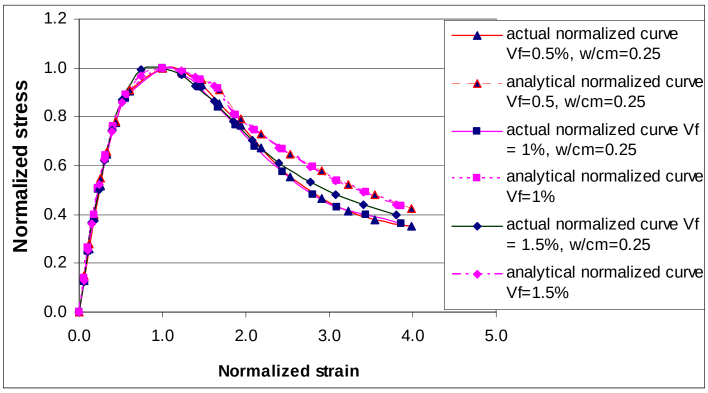

Fig. 13 Correlation of normalized actual and analytical curves for various fiber volume fractions and *w*/cm=0.25)

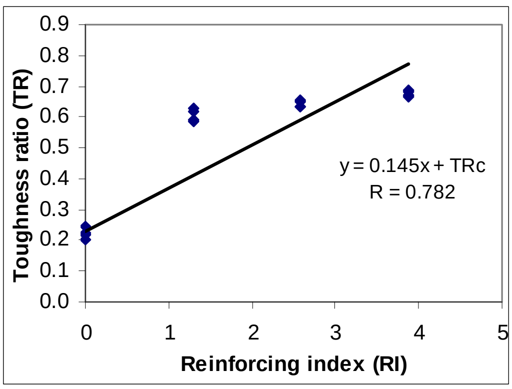

Fig. 14 Toughness ratio of SFRC as function of fiber reinforcing index and toughness ratio of plain concrete

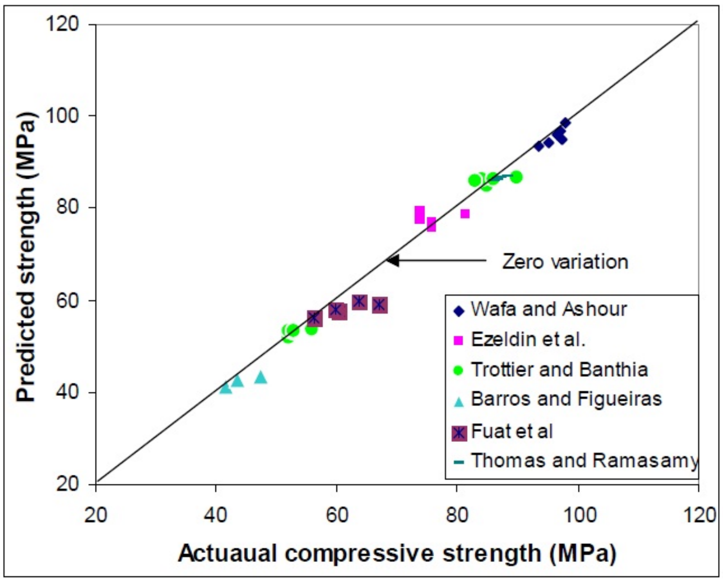

Fig. 15 Comparison of strength data of various researchers with the predicted compressive strength (MPa) of the present model

The above equations can be used for fiber reinforcing index up to 3.9 for the crimped steel fiber.

For a given plain concrete strength and RI = w_f* (l/d), the engineering properties, E_{it}, f_o and ε_o are calculated using Eqs. (1), (4) and (5). These values are then inserted in to Eq. (8) to obtain β the dimensionless parameter. The proposed Eq. (5) can be used to evaluate the strain for SFRC, using a value of 0.002 for strain (ε) which has been accepted widely as constant for plain concrete (CEB-FIB code 1991). With the values β and ε_o being known, ascending branch of the stress-strain (σ–ε) curve may be generated using Eq. (7) while with the value of RI and β from Eq. (9c) and ε_o being known, the descending branch of the curve is obtained from Eq. (8). Thus, the proposed model fits the post-peak softening behavior. The descending part of the σ-ε curves is effected by β value. The area under σ–ε curve increases as the β value decreases which means the curve becomes flatter (Figs. 3-7). Ezheldin and Balaguru (1992) have suggested a correction factor to generate σ–ε curves for the full length or middle third length of the measurements, may be used. The whole length of the cylinder for deformation measurements is used in this article.

The predictions using this proposed analytical model are thus computed and compared with the experimental values, are in good agreement with the experimental curves even with the global averaging of the key parameters. Correlation of normalized actual and analytical stress-strain curves for various fiber volume fractions and w/cm ratio = 0.25 are shown in Fig. 13, in which the accuracy of the model developed is revealed. Thus, the proposed model (Eq. (7)) can be used to obtain the complete stress-strain (σ–ε) curve of HPFRC containing crimped fiber. The parameters needed are the reinforcing index RI, the peak strength of fibrous concrete and the corresponding strain.

6. Conclusions

The following conclusions may be drawn from the experimental and analytical study on the compression behavior of HPSFRC.

1. The addition of crimped steel fibers to HPC matrix chances the basic characteristics of its stress-strain behavior. The slope of the descending branch increases with increasing the fiber content.
2. The compressive toughness and ductility were increased considerably due to the addition of fibers in HPC mixes. The increase in toughness is directly proportional to the reinforcing index (RI). A moderate increase in compressive strength and increase in strain at peak stress were also observed, which are proportional to the reinforcing index (RI).
3. An analytical expression is proposed to generate the complete σ-*ε* curves for the HPFRC based on the non-dimensional parameter '*β*' and strain corresponding to the peak compressive stress. This expression is valid for crimped steel-fiber with fiber reinforcing index (RI) up to 3.9.
4. The toughness ratio computed from the σ–*ε* curves based on the prediction equation, matches with values calculated from the experimental results.
5. The Carriera and Chu equation, as modified herein by introducing the parameter *β* (Eq. 9c) for the descending branch, gives good predictions of the complete stress-strain response of HPSFRC.

References

ACI Committee 211 (1999), *Guide for selecting proportions for high strength concrete with Portland cement and fly ash*, ACI 211.4R-93, *ACI Manual of concrete practice*, Farmington Hills.

ACI Committee 211 (1999), *Standard practice for selecting proportions for normal, heavy weight and mass concrete*, ACI 211.1-91, *ACI Manual of concrete practice*, Farmington Hills.

ACI Committee 544 (2006), *Design considerations for steel fiber reinforced concrete*, ACI 544.4R-89, *American Concrete Institute*, Detroit.

ACI Committee 544 (2006), *Guide for specifying, mixing, placing and finishing steel fiber reinforced concrete*, ACI 544.3R- 93, *American Concrete Institute*, Detroit.

ACI Committee 544 (2006), *State-of-the-art report on fiber reinforced concrete*, ACI 544.1R- 82, *American Concrete Institute*, Detroit.

Aitcin, P.C. (1998), *High strength concrete*, Spon press, London (UK).

ASTM C39-1992 (1999), *Standard test method for compressive strength of fiber reinforced concrete*, *Annual book of ASTM standards*, American Society for Testing and Materials.

ASTM C78-1992 (1992), *Standard test method for flexural strength of fiber reinforced concrete*, *Annual book of ASTM standards*, American society for testing and materials.

Balaguru, N. and Shah, S.P. (1992), *Fiber reinforced concrete composites*, McGraw Hill.

Bang, Y.L., Jin-Keun, K. and Yun, Y.K. (2010), "Prediction of ECC tensile stress-strain curves based on modified fiber bridging relations considering fiber distribution characteristics", *Comput. Concrete,* **7**(5), 455-468.

Barros, J.A.O. and Figueiras, J.A. (1999), "Flexural behavior of SFRC: Testing and modeling", *J. Mater Civil. Eng.,* **11**(4), 331-339.

Bhargava, P., Sharma, U.K. and Kaushik, S.K. (2006), "Compressive stress-strain behavior of small scale steel fiber reinforced high strength concrete cylinders", *J. Adv. Concrete Technol.*, **4**(1), 109-121.

Campione, G. and Mendola, L.L. (2004), "Behavior in compression of light weight fiber reinforced concrete confined with transverse steel reinforcement", *Cement Concrete Comp.*, **26**(6), 645-656.

Carriera, D.J. and Chu, K.H. (1985), "Stress-strain relationship for plain concrete in compression", *ACI J.*, **82**(6), 797-804.

Chin, M.S., Mansur, M.A. and Wee, Y.H. (1997), "Effects of shape, size and casting direction of specimens on stress-strain curves of high strength concrete", *ACI Mater. J.*, **94**(3), 209-219.

Ezheldin, A.S. and Balaguru, P.N. (1992), "Normal and high strength fiber reinforced concrete under compression", *J. Mater. Civil Eng*., **4**(4), 415-429.
Fuat, K., Faith. A. and Ilhami, Y. (2008), "Combined effects of silica fume and steel fiber on the mechanical properties of high-strength concrete", *Constr. Build. Mater.*, **22**(8), 1874-1880.
Haktanir, T., Ari, K., Altum, F. and Karahan, D. (2006), "Effect of steel fibers and mineral filler on the water tightness of concrete pipes", *Cement Concrete Comp.*, **28**(10), 811-816.
Hsu, L.S. and Hsu, C.T. (1994), "Stress-strain behavior of steel fiber reinforced high-strength concrete under compression", *ACI Struct. J.*, **91**(4), 448-457.
Ismail, H.C. and Riza, D. (2011), "Modeling of concrete containing steel fibers: toughness and mechanical properties", *Comput. Concrete,* **8**(3), 357-369.
Thomas, J. and Ramasamy, A. (2007), "Mechanical properties of steel fiber reinforced concrete", *J. Mater. Civil Eng*., **19**(5), 385-392.
Kittinun, S., Sherif, E.T. and Gastavo, P.M. (2010), "Behavior of high performance fiber reinforced cement composite under multi-axial compressive loading", *Cement Concrete Comp.*, **32**(1), 62-72.
Mansur, M.A., Chin, M.S. and Wee, Y.H. (1999), "Stress-strain relationship of high strength fiber concrete in compression", *J. Mater. Civil Eng*., **13**(1), 21-29.
Nataraja, M.C., Dhang, N. and Gupta, A.P. (1999), "Stress-strain curve for steel fiber reinforced concrete in compression", *Cement Concrete Comp.*, **21**(5/6), 383-390.
Ramadoss, P. and Nagamani, K. (2008), "A new strength model for the high-performance fiber reinforced concrete", *Comput. Concrete*, **5**(1), 21-36.
Ramesh, K., Seshu, D.R. and Prabhakar, M. (2003), "Constitutive behavior of confined fiber reinforced concrete under axial compression", *Cement Concrete Comp.*, **25**(3), 343-350.
Trottier, J. and Banthia, N. (1994), "Toughness characteristics of steel-fiber reinforced concrete", *J. Mater. Civil Eng*., **6**(2), 264-289.
Wafa, F.F. and Ashour, S.A. (1992), "Mechanical properties of high- strength fiber reinforced concrete", *ACI Mater. J.*, **89**(5), 445-455.
Wang, P.T., Shah, S.P. and Naaman, A.N. (1997), "Stress-strain curve of normal and light- weight concrete in compression", *ACI Mater. J.*, **75**(11), 603-611.
Wang, Z., Liu, Y.S. and Shen, R.F. (2008), "Stress-strain relationship of steel fiber reinforced concrete under dynamic compression", *Constr. Build. Mater.*, **22**(5), 811-819.
Wee, Y.H., Chin, M.S. and Mansur, M.A. (1996), "Stress-strain relationship of high strength concrete in compression", *J. Mater. Civil Eng*., **8**(2), 70-76.
Williams, E.M., Graham, S.S. and Rusting, T.S. (2010) "Constitutive property behavior of an ultra HPC with and without steel fibers", *Comput. Concrete*, **7**(2), 192-202.
Xu, B.W. and Shi, H.S. (2009), "Correlations among mechanical properties of steel fiber reinforced concrete", *Constr. Build. Mater.*, **23**(12), 3468-3474.
Zongjin, L. and Yanhua, Z. (2010), "Obtaining equivalent fracture toughness of concrete using uniaxial compression test", *Comput. Concrete*, **7**(4), 387-402.

CC

Notations

HPSFRC= high-performance steel fiber reinforced concrete
f'_{cf} or f_o = cylinder compressive strength of HPSFRC, MPa
f'_c = compressive strength of plain concrete (HPC), MPa
f_{rf} = modulus of rupture of HPSFRC, MPa
ε_o= strain corresponding to peak stress of HPSFRC, mm/mm
ε_c= strain corresponding to peak stress of HPC, mm/mm
TR_f =toughness ratio of HPSFRC
TR_c =toughness ratio of HPC
E_{it} = initial tangent modulus, MPa
E_c = secant modulus of elasticity, MPa
V_f = volume fraction of steel fiber, percent
$_{wf}$ = weight fraction
l/d = aspect ratio of fiber
RI= fiber reinforcing index.